Journal of Science and Technology in Civil Engineering NUCE 2019. 13 (3): 34–44

RITZ SOLUTION FOR BUCKLING ANALYSIS OF THIN-WALLED COMPOSITE CHANNEL BEAMS BASED ON A CLASSICAL BEAM THEORY

Nguyen Ngoc Duong[a,*], Nguyen Trung Kien[a], Nguyen Thien Nhan[b]

[a] *Faculty of Civil Engineering, HCMC University of Technology and Education, No 1 Vo Van Ngan street, Thu Duc district, Ho Chi Minh city, Vietnam*
[b] *Faculty of Engineering and Technology, Kien Giang University, 320A Route 61, Chau Thanh district, Kien Giang province, Vietnam*

Article history:
Received 05/08/2019, Revised 28/08/2019, Accepted 30/08/2019

Abstract

Buckling analysis of thin-walled composite channel beams is presented in this paper. The displacement field is based on classical beam theory. Both plane stress and plane strain state are used to achieve constitutive equations. The governing equations are derived from Lagrange's equations. Ritz method is applied to obtain the critical buckling loads of thin-walled beams. Numerical results are compared to those in available literature and investigate the effects of fiber angle, length-to-height's ratio, boundary condition on the critical buckling loads of thin-walled channel beams.

Keywords: Ritz method; thin-walled composite beams; buckling.

https://doi.org/10.31814/stce.nuce2019-13(3)-04

1. Introduction

Composite materials are widely used in many fields of civil, aeronautical and mechanical engineering owing to low thermal expansion, enhanced fatigue life, good corrosive resistance, and high stiffness-to-weight and strength-to-weight ratios. A large number of structural members made of composites have the form of thin-walled beams. In addition to the increasing in application, thin-walled composite beams also attract a huge attention from reseachers to study their structural behaviours.

The thin-walled theories are presented by [1, 2]. Bauld and Lih-Shyng [3] then developed Vlasov's thin-walled isotropic material beam theory for the composite one. Gupta et al. [4] used finite element method (FEM) for analysing thin-walled Z-section laminated anisotropic beams. Bank and Bednarczyk [5] proposed a thin-walled beam theory for bending analysis of composite beams by considering shear deformation. In this study, the Timoshenko beam theory together with a modified form of the shear coefficient are developed. An analytical study for flexural-torsional stability of thin-walled composite I-beams is presented by [6, 7]. Based on FEM and classical lamination theory, [8–10] predicted flexural-torsional buckling load of thin-walled composite beams. Navier solution is used by [11] for buckling and free vibration analysis of thin-walled composite beams. Shan and Qiao [12] conducted a combined analytical and experimental study for buckling behaviours of composite channel beams by considering the bending-twisting coupling and shear effect. Cortinez and Piovan [13] used FEM

[*]Corresponding author. *E-mail address:* duongnn@hcmute.edu.vn (Duong, N. N.)

for the stability analysis of thin-walled composite beams. The displacement fields in this study are developed by using non-linear theory. The exact stiffness matrix method are proposed by [14, 15] for flexural-torsional stability analysis of thin-walled composite I-beams. Vo and Lee [16, 17] used FEM for flexural-torsional stability analysis of thin-walled composite beams. In recent years, buckling behaviours of thin-walled functionally grade open section beams are also analysed [18–21]. It can be seen that Ritz method has seldom been used to analyse the buckling problem of thin-walled composite channel beams.

In this paper, the bending and warping shears are considered. The main novelty of this paper is to apply a Ritz solution for the buckling analysis of thin-walled composite beams. The governing equations are derived by using Lagrange's equations. Results of the present element are compared with those in available literature to show its accuracy of the present solution. Parametric study is also performed to investigate the effects of length-to-height ratio, fibre angle on critical buckling loads of the thin-walled composite beams.

2. Theoretical formulation

The theoretical development requires three sets of coordinate systems as shown in Fig. 1. The first coordinate system is the orthogonal Cartesian coordinate system (x, y, z), for which the y- and z-axes lie in the plane of the cross-section and the x axis parallel to the longitudinal axis of the beam. The second coordinate system is the local plate coordinate (n, s, x) wherein the n axis is normal to the middle surface of a plate element, the s axis is tangent to the middle surface and is directed along the contour line of the cross-section. θ_s is an angle of orientation between (n, s, x) and (x, y, z) coordinate systems. The pole P, which has coordinate (y_P, z_P), is called the shear center [22].

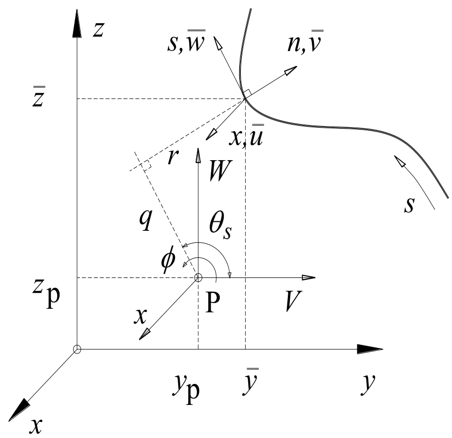

Figure 1. Thin-walled coordinate systems

2.1. Constitutive relations

The constitutive equations for the k^{th}-ply in the global coordinate system (n, s, x) are given by:

$$\begin{Bmatrix} \sigma_x \\ \sigma_s \\ \sigma_{xs} \end{Bmatrix}^{(k)} = \begin{pmatrix} \bar{Q}_{11} & \bar{Q}_{12} & \bar{Q}_{16} \\ \bar{Q}_{12} & \bar{Q}_{22} & \bar{Q}_{26} \\ \bar{Q}_{16} & \bar{Q}_{26} & \bar{Q}_{66} \end{pmatrix}^{(k)} \begin{Bmatrix} \varepsilon_x \\ \varepsilon_s \\ \gamma_{xs} \end{Bmatrix} \tag{1}$$

where $\bar{Q}_{ij}$ are transformed reduced stiffnesses. The one-dimensional stress states of thin-walled composite beams are derived from Eq. (1) by assuming plane strain or plane stress state [23, 24]:

$$\begin{Bmatrix} \sigma_x \\ \sigma_{xs} \end{Bmatrix}^{(k)} = \begin{pmatrix} \bar{\bar{Q}}_{11} & \bar{\bar{Q}}_{16} \\ \bar{\bar{Q}}_{16} & \bar{\bar{Q}}_{66} \end{pmatrix}^{(k)} \begin{Bmatrix} \varepsilon_x \\ \gamma_{xs} \end{Bmatrix} \tag{2}$$

- For plane strain state ($\varepsilon_s = 0$):

$$\bar{\bar{Q}}_{11} = \bar{Q}_{11}, \bar{\bar{Q}}_{16} = \bar{Q}_{16}, \bar{\bar{Q}}_{66} = \bar{Q}_{66} \tag{3}$$

- For plane stress state ($\sigma_s = 0$):

$$\bar{\bar{Q}}_{11} = \bar{Q}_{11} - \frac{\bar{Q}_{12}^2}{\bar{Q}_{22}}, \bar{\bar{Q}}_{16} = \bar{Q}_{16} - \frac{\bar{Q}_{12}\bar{Q}_{26}}{\bar{Q}_{22}}, \bar{\bar{Q}}_{66} = \bar{Q}_{66} - \frac{\bar{Q}_{26}^2}{\bar{Q}_{22}} \tag{4}$$

Constitutive equation in Eq. (2) can be also applied for thin-walled isotropic beams [25]:

$$\bar{\bar{Q}}_{11} = E, \bar{\bar{Q}}_{16} = 0, \bar{\bar{Q}}_{66} = G = \frac{E}{2(1+\upsilon)} \tag{5}$$

where E, G and υ are Young's modulus, shear modulus and Poisson ratio of isotropic material, respectively.

2.2. Kinematics

The mid-surface displacements $(\bar{u}, \bar{v}, \bar{w})$ at a point in the contour coordinate system are written by [26, 27]:

$$\bar{v}(s,x) = V(x)\sin\theta_s(s) - W(x)\cos\theta_s(s) - \phi(x)q(s) \tag{6}$$

$$\bar{w}(s,x) = V(x)\cos\theta_s(s) + W(x)\sin\theta_s(s) + \phi(x)r(s) \tag{7}$$

$$\bar{u}(s,x) = U(x) - V_{,x}(x)y(s) - W_{,x}(x)z(s) - \psi_{\varpi}(x)\varpi(s) \tag{8}$$

where the comma symbol indicates a partial differentiation with respect to the corresponding subscript coordinate. U, V and W are displacement of P in the x-, y- and z- directions, respectively; ϕ is the rotation angle about pole axis; ϖ is warping function given by:

$$\varpi(s) = \int_{s_0}^{s} r(s)ds \tag{9}$$

It can be seen that displacement fields in Eqs. (6)–(8) are derived from Vlasov assumption which shear strain of the mid-surface is zero in each plate $\left(\bar{\gamma}_{sx} = \frac{\partial\bar{w}}{\partial x} + \frac{\partial\bar{u}}{\partial s} = 0\right)$ [1, 27]. The displacements (u, v, w) at any generic point on section are obtained from Kirchhoff–Love's the classical plate theory which ignored shear deformation [27]:

$$v(n,s,x) = \bar{v}(s,x) \tag{10}$$

$$w(n,s,x) = \bar{w}(s,x) - n\bar{v}_{,s}(s,x) \tag{11}$$

$$u(n,s,x) = \bar{u}(s,x) - n\bar{v}_{,x}(s,x) \tag{12}$$

The strains fields are obtained:

$$\varepsilon_x = \bar{\varepsilon}_x + n\bar{\kappa}_x \tag{13}$$

$$\gamma_{sx} = n\bar{\kappa}_{sx} \tag{14}$$

where

$$\bar{\varepsilon}_x = \frac{\partial\bar{u}}{\partial x}, \bar{\kappa}_x = -\frac{\partial^2\bar{v}}{\partial x^2}, \bar{\kappa}_{sx} = -2\frac{\partial^2\bar{v}}{\partial s\partial x} \tag{15}$$

In Eq. (15), $\bar{\varepsilon}_x, \bar{\kappa}_x$ and $\bar{\kappa}_{sx}$ are mid-surface axial strain and biaxial curvature of the plate, respectively. Thin-walled beam strain fields can be obtained by substituting Eqs. (6)–(8) into Eq. (15) as:

$$\bar{\varepsilon}_x = \varepsilon_x^0 + y\kappa_z + z\kappa_y + \varpi\kappa_\varpi \tag{16}$$

$$\bar{\kappa}_x = \kappa_z \sin\theta - \kappa_y \cos\theta - \kappa_\varpi q \tag{17}$$

$$\bar{\kappa}_{sx} = \kappa_{sx} \tag{18}$$

where $\varepsilon_x^0, \kappa_y, \kappa_z, \kappa_\varpi, \kappa_{sx}$ are axial strain, biaxial curvatures in the y and z direction, warping curvature with respect to the shear center, and twisting curvature in the beam, respectively defined as:

$$\varepsilon_x^0 = U_{,x} \tag{19}$$

$$\kappa_y = -W_{,xx} \tag{20}$$

$$\kappa_z = -V_{,xx} \tag{21}$$

$$\kappa_\varpi = -\phi_{,xx} \tag{22}$$

$$\kappa_{sx} = -2\phi_{,x} \tag{23}$$

Substituting Eqs. (16)–(23) into Eqs. (13)–(14), the strains fields of thin-walled beam can be written as:

$$\varepsilon_x = \varepsilon_x^0 + (y + n\sin\theta)\,\kappa_z + (z - n\cos\theta)\,\kappa_y + (\varpi - nq)\,\kappa_\varpi \tag{24}$$

$$\gamma_{sx} = n\kappa_{sx} \tag{25}$$

2.3. Variational formulation

The strain energy Π_E of the beam is given by:

$$\begin{aligned}\Pi_E &= \frac{1}{2}\int_\Omega (\sigma_x\varepsilon_x + \sigma_{sx}\gamma_{sx})d\Omega \\ &= \frac{1}{2}\int_0^L \Big(E_{11}U_{,x}^2 - 2E_{12}U_{,x}V_{,xx} - 2E_{13}U_{,x}W_{,xx} - 4E_{14}U_{,x}\phi_{,x} + E_{22}V_{,xx}^2 + 2E_{24}V_{,xx}\phi_{,xx} \\ &+E_{33}W_{,xx}^2 + 2E_{34}W_{,xx}\phi_{,xx} - 4E_{35}W_{,xx}\phi_{,x} + E_{44}\phi_{,xx}^2 + 4E_{55}\phi_{,x}^2\Big)\,dx\end{aligned} \tag{26}$$

where Ω is volume of beam, E_{ij} is stiffness of thin-walled composite beam (see [9] for more detail).

The potential energy Π_W of thin-walled beam subjected to axial compressive load N_0 can be expressed as:

$$\begin{aligned}\Pi_W &= -\frac{1}{2}\int_\Omega \frac{N_0}{A}\left(v_{,x}^2 + w_{,x}^2\right)d\Omega \\ &= -\frac{1}{2}\int_0^L N_0\left(V_{,x}^2 + W_{,x}^2 + 2z_pV_{,x}\phi_{,x} - 2y_pW_{,x}\phi_{,x} + \frac{I_P}{A}\phi_{,x}^2\right)dx\end{aligned} \tag{27}$$

where A is the cross-sectional area, I_P is polar moment of inertia of the cross-section about the centroid defined by [8, 18]:

$$I_P = I_y + I_z \tag{28}$$

where I_y and I_z are second moment of inertia with respect to y- and z-axis, respectively, given by:

$$I_y = \int_A z^2 dA \tag{29}$$

$$I_z = \int_A y^2 dA \tag{30}$$

The total potential energy of thin-walled beam is expressed by:

$$\begin{aligned}\Pi &= \Pi_E + \Pi_W \\ &= \frac{1}{2}\int_0^L \Big(E_{11}U_{,x}^2 - 2E_{12}U_{,x}V_{,xx} - 2E_{13}U_{,x}W_{,xx} - 4E_{14}U_{,x}\phi_{,x} + E_{22}V_{,xx}^2 + 2E_{24}V_{,xx}\phi_{,xx} \\ &+E_{33}W_{,xx}^2 + 2E_{34}W_{,xx}\phi_{,xx} - 4E_{35}W_{,xx}\phi_{,x} + E_{44}\phi_{,xx}^2 + 4E_{55}\phi_{,x}^2\Big)\,dx \\ &- \frac{1}{2}\int_0^L N_0\left(V_{,x}^2 + W_{,x}^2 + 2z_pV_{,x}\phi_{,x} - 2y_pW_{,x}\phi_{,x} + \frac{I_P}{A}\phi_{,x}^2\right)dx\end{aligned} \tag{31}$$

2.4. Ritz solution

By using the Ritz method, the displacement field is approximated by:

$$U(x) = \sum_{j=1}^m \varphi_{j,x}(x)U_j \tag{32}$$

$$V(x) = \sum_{j=1}^m \varphi_j(x)V_j \tag{33}$$

$$W(x) = \sum_{j=1}^m \varphi_j(x)W_j \tag{34}$$

$$\phi(x) = \sum_{j=1}^m \varphi_j(x)\phi_j \tag{35}$$

where U_j, V_j, W_j and ϕ_j are unknown and need to be determined; $\varphi_j(x)$ are approximation functions [21]. It should be noted that these approximation functions in Table 1 satisfy the various boundary conditions (BCs) such as simply-supported (S-S), clamped-free (C-F), clamped-simply supported (C-S) and clamped-clamped (C-C).

By substituting Eqs. (32)–(35) into Eq. (31) and using Lagrange's equations:

$$\frac{\partial \Pi}{\partial p_j} = 0 \tag{36}$$

with p_j representing the values of $\left(U_j, V_j, W_j, \phi_j\right)$, the buckling behaviours of the thin-walled beam can be obtained by solving the following equations:

$$\left(\begin{bmatrix} \mathbf{K}^{11} & \mathbf{K}^{12} & \mathbf{K}^{13} & \mathbf{K}^{14} \\ {}^T\mathbf{K}^{12} & \mathbf{K}^{22} & \mathbf{K}^{23} & \mathbf{K}^{24} \\ {}^T\mathbf{K}^{13} & {}^T\mathbf{K}^{23} & \mathbf{K}^{33} & \mathbf{K}^{34} \\ {}^T\mathbf{K}^{14} & {}^T\mathbf{K}^{24} & {}^T\mathbf{K}^{34} & \mathbf{K}^{44} \end{bmatrix}\right)\begin{Bmatrix} \mathbf{u} \\ \mathbf{v} \\ \mathbf{w} \\ \mathbf{\Phi} \end{Bmatrix} = \begin{Bmatrix} \mathbf{0} \\ \mathbf{0} \\ \mathbf{0} \\ \mathbf{0} \end{Bmatrix} \tag{37}$$

Table 1. Approximation functions and essential BCs of thin-walled beams

BC	$\dfrac{\varphi_j(x)}{e^{\frac{-jx}{L}}}$	$x=0$	$x=L$
S-S	$\dfrac{x}{L}\left(1-\dfrac{x}{L}\right)$	$V=W=\phi=0$	$V=W=\phi=0$
C-F	$\left(\dfrac{x}{L}\right)^2$	$U=V=W=\phi=0$	$V_{,x}=W_{,x}=\phi_{,x}=0$
C-S	$\left(\dfrac{x}{L}\right)^2\left(1-\dfrac{x}{L}\right)$	$U=V=W=\phi=0$, $V_{,x}=W_{,x}=\phi_{,x}=0$	$V=W=\phi=0$
C-C	$\left(\dfrac{x}{L}\right)^2\left(1-\dfrac{x}{L}\right)^2$	$U=V=W=\phi=0$, $V_{,x}=W_{,x}=\phi_{,x}=0$	$U=V=W=\phi=0$, $V_{,x}=W_{,x}=\phi_{,x}=0$

where the stiffness matrix $\mathbf{K}$ is given by:

$$\begin{aligned}
K_{ij}^{11} &= E_{11}\int_0^L \varphi_{i,xx}\varphi_{j,xx}dx,\quad K_{ij}^{12} = -E_{12}\int_0^L \varphi_{i,xx}\varphi_{j,xx}dx,\quad K_{ij}^{13} = -E_{13}\int_0^L \varphi_{i,xx}\varphi_{j,xx}dx,\\
K_{ij}^{14} &= 2E_{15}\int_0^L \varphi_{i,xx}\varphi_{j,x}dx - E_{14}\int_0^L \varphi_{i,xx}\varphi_{j,xx}dx,\quad K_{ij}^{22} = E_{22}\int_0^L \varphi_{i,xx}\varphi_{j,xx}dx + N_0\int_0^L \varphi_{i,x}\varphi_{j,x}dx,\\
K_{ij}^{23} &= E_{23}\int_0^L \varphi_{i,xx}\varphi_{j,xx}dx,\quad K_{ij}^{24} = E_{24}\int_0^L \varphi_{i,xx}\varphi_{j,xx}dx - 2E_{25}\int_0^L \varphi_{i,xx}\varphi_{j,x}dx + N_0 z_p\int_0^L \varphi_{i,x}\varphi_{j,x}dx,\\
K_{ij}^{33} &= E_{33}\int_0^L \varphi_{i,xx}\varphi_{j,xx}dx,\quad K_{ij}^{34} = E_{34}\int_0^L \varphi_{i,xx}\varphi_{j,xx}dx - 2E_{35}\int_0^L \varphi_{i,xx}\varphi_{j,x}dx - N_0 y_p\int_0^L \varphi_{i,x}\varphi_{j,x}dx,\\
K_{ij}^{44} &= E_{44}\int_0^L \varphi_{i,xx}\varphi_{j,xx}dx - 2E_{45}\int_0^L \left(\varphi_{i,xx}\varphi_{j,x}+\varphi_{i,x}\varphi_{j,xx}\right)dx + 4E_{55}\int_0^L \varphi_{i,x}\varphi_{j,x}dx + \frac{N_0 I_p}{A}\int_0^L \varphi_{i,x}\varphi_{j,x}dx
\end{aligned} \tag{38}$$

3. Numerical results

In this section, numerical results are carried out to determine critical buckling loads of thin-walled channel beams with various configurations including boundary conditions, lay-ups. The material properties and geometry of thin-walled beams are given in Table 2 and Fig. 2.

Firstly, in order to verify the present solution, a simply-supported beam with isotropic channel section ($b_1 = b_2 = 14.5$ cm, $b_3 = 30$ cm, $h_1 = h_2 = h_3 = 1.0$ cm, $E = 200$ GPa and $G = 80$ GPa)

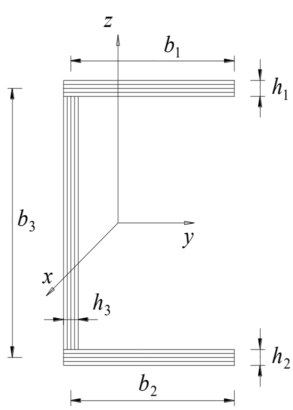

Figure 2. Geometry of thin-walled composite channel beams

Table 2. Material properties of thin-walled beams

Material (MAT) properties	MAT.I	MAT.II
E_1 (GPa)	144	141.9
$E_2 = E_3$ (GPa)	9.65	9.78
$G_{12} = G_{13}$ (GPa)	4.14	6.13
G_{23} (GPa)	3.45	4.8
$\nu_{12} = \nu_{13}$	0.30	0.42

is considered. The critical buckling load is presented in Table 3. It is clear that the present results are coincided with those obtained from [18]. Another verified example is also performed for composite beams. The critical buckling load of channel beams (MAT.I, $b_1 = b_2 = b_3 = 10$ cm, $h_1 = h_2 = h_3 = 1.0$ cm and $L = 20b_3$) is showed in Table 4 and compared with [13]. Good agreement is also found. It should be noted that the buckling load for plane strain state ($\varepsilon_s = 0$) is bigger for plane stress state ($\sigma_s = 0$). This phenomenon can be explained by the fact that the plane strain state is equivalent ignoring Poisson's effect and causes the beams stiffer.

Table 3. Critical buckling load (kN) of simply-supported beam

L (m)	Reference		Note
	Present	Nguyen et al. [18]	
4	1569.64	1552.57	Torsional buckling
6	772.43	772.43	Flexural buckling
8	434.50	434.50	Flexural buckling

Table 4. Critical buckling load (10^5 N) of thin-walled channel beams

BC	Reference	Lay-up	
		$(0^0/0^0/0^0/0^0)$	$(0^0/90^0/90^0/0^0)$
S-S	Present ($\varepsilon_s = 0$)	2.631	1.603
	Present ($\sigma_s = 0$)	2.617	1.595
	Cortinez and Piovan [13]	2.674	1.635
C-F	Present ($\varepsilon_s = 0$)	0.932	0.658
	Present ($\sigma_s = 0$)	0.929	0.656
	Cortinez and Piovan [13]	0.947	0.670
C-S	Present ($\varepsilon_s = 0$)	4.979	2.884
	Present ($\sigma_s = 0$)	4.952	2.869
	Cortinez and Piovan [13]	5.058	2.941
C-C	Present ($\varepsilon_s = 0$)	9.364	5.270
	Present ($\sigma_s = 0$)	9.310	5.240
	Cortinez and Piovan [13]	9.503	5.371

Secondly, the symmetric angle-ply channel beams with the various BCs and lay-ups are considered. The thickness of flanges and web are of 0.0762 cm, and made of asymmetric laminates that consist of 6 layers ($[\eta - \eta]_3$). The critical buckling load of channel beams (MAT.II, $b_1 = b_2 = 0.6$ cm, $b_3 = 2.0$ cm and $L = 100b_3$) is showed in Table 5. It can be observed that the buckling load reduces as lay-up increases for all BCs. From Table 5, it can be seen that there is a significant difference between results of plane stress and plane strain state for beams with arbitrary angle. Available literatures indicate that plane stress assumption is more appropriate and widely used for composite beams [23, 24, 28–30]. Figs. 3(a)–3(f) show first three buckling mode shape of S-S beams with $[30/-30]_3$ angle-fly in flanges and web. It can be seen that the buckling mode 1, 2 and 3 are first flexural mode in y-direction (Mode V), first and second torsional mode (Mode Φ) for both plane stress and plane strain state.

Table 5. Critical buckling load (N) of thin-walled channel beams

BC	Lay-up						
	[0]	$[15/-15]$	$[30/-30]$	$[45/-45]$	$[60/-60]$	$[75/-75]$	$[90/-90]$
S-S							
$\varepsilon_s = 0$	28.215	24.944	17.172	9.137	4.062	2.222	1.945
$\sigma_s = 0$	27.871	22.572	10.379	4.180	2.456	2.011	1.921
C-F							
$\varepsilon_s = 0$	7.054	6.206	4.263	2.269	1.011	0.555	0.486
$\sigma_s = 0$	6.968	5.618	2.581	1.042	0.614	0.503	0.480
C-S							
$\varepsilon_s = 0$	57.720	50.864	34.951	18.598	8.283	4.543	3.978
$\sigma_s = 0$	57.018	46.038	21.152	8.532	5.022	4.113	3.930
C-C							
$\varepsilon_s = 0$	112.858	99.383	68.257	36.320	16.183	8.881	7.778
$\sigma_s = 0$	111.486	89.958	41.322	16.673	9.817	8.043	7.684

Finally, effect of length-to-height ratio on buckling behaviours of the thin-walled composite beams is investigated. Figs. 4(a) and 4(b) show the critical buckling load of beams (MAT.II, $b_1 = b_2 = 0.6$ cm, $b_3 = 2.0$ cm, $h_1 = h_2 = h_3 = 0.0762$ cm and $[45/-45]_3$). It can be seen that the buckling load reduces as length-to-height ratio increases for all BCs.

4. Conclusions

Ritz method is applied to analyse buckling of thin-walled composite channel beams in this paper. The theory is based on the classical theory. The governing equations are derived from Lagrange's equations. The critical buckling loads of thin-walled composite channel beams with various BCs are obtained and compared with those of the previous works. The results indicate that:

- The effects of fiber orientation are significant for buckling behaviours of thin-walled channel beams.

- For thin-walled beams with arbitrary angle, the buckling loads for plane stress and for plane strain state are significantly different.

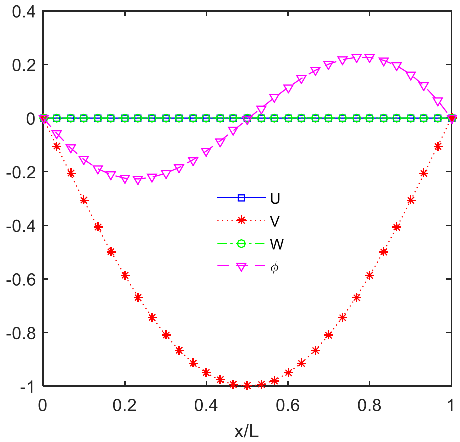

(a) Mode shape 1: N_{01} = 17.172 N ($\varepsilon_s = 0$)

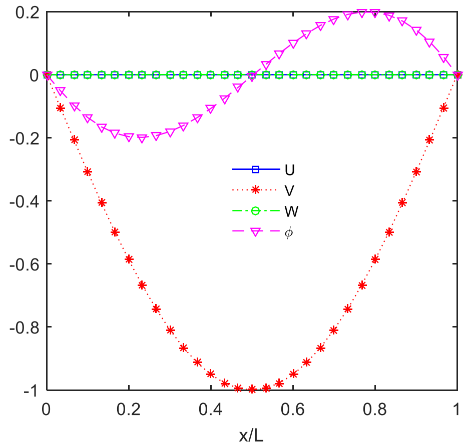

(b) Mode shape 1: N_{01} = 10.379 N ($\sigma_s = 0$)

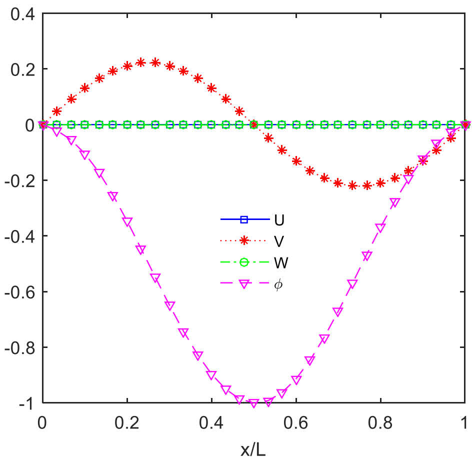

(c) Mode shape 2: N_{02} = 68.171 N ($\varepsilon_s = 0$)

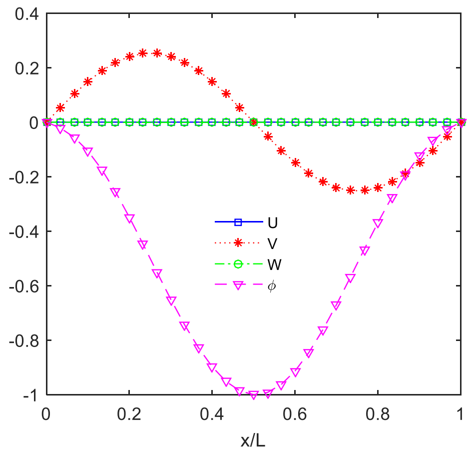

(d) Mode shape 2: N_{02} = 41.283 N ($\sigma_s = 0$)

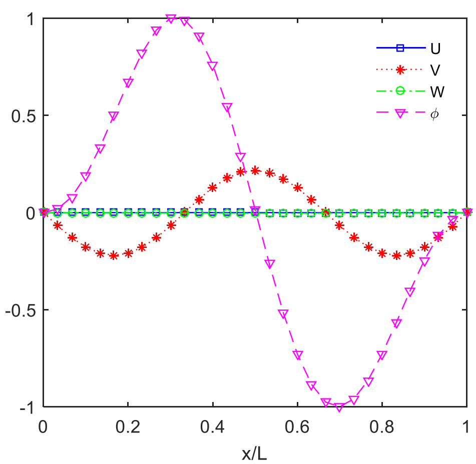

(e) Mode shape 3: N_{03} = 153.482 N ($\varepsilon_s = 0$)

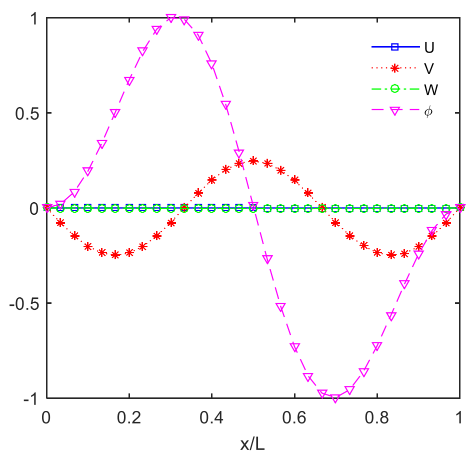

(f) Mode shape 3: N_{03} = 92.949 N ($\sigma_s = 0$)

Figure 3. First three buckling mode shape of S-S beams

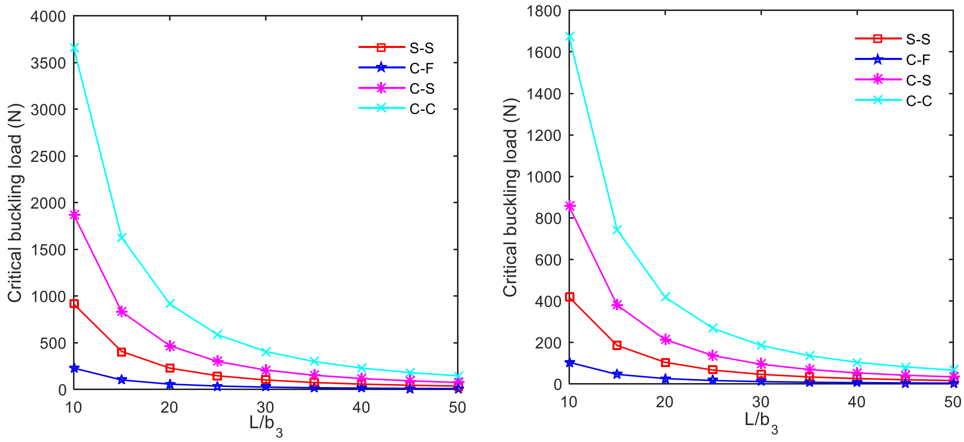

(a) $\varepsilon_s = 0$ (b) $\sigma_s = 0$

Figure 4. Critical buckling load of thin-walled composite channel beams

- The present solution is found to be appropriate and efficient in analysing buckling problems of thin-walled composite channel beams.

Acknowledgment

This research is funded by Vietnam National Foundation for Science and Technology Development (NAFOSTED) under grant number 107.02-2018.312.

References

[1] Vlasov, V. (1961). *Thin-walled elastic beams*. Israel program for scientific translations, Jerusalem.

[2] Gjelsvik, A. (1981). *The theory of thin walled bars*. Krieger Pub Co.

[3] Bauld Jr, N. R., Lih-Shyng, T. (1984). A Vlasov theory for fiber-reinforced beams with thin-walled open cross sections. *International Journal of Solids and Structures*, 20(3):277–297.

[4] Gupta, R. K., Venkatesh, A., Rao, K. P. (1985). Finite element analysis of laminated anisotropic thin-walled open-section beams. *Composite Structures*, 3(1):19–31.

[5] Bank, L. C., Bednarczyk, P. J. (1988). A beam theory for thin-walled composite beams. *Composites Science and Technology*, 32(4):265–277.

[6] Pandey, M. D., Kabir, M. Z., Sherbourne, A. N. (1995). Flexural-torsional stability of thin-walled composite I-section beams. *Composites Engineering*, 5(3):321–342.

[7] Sherbourne, A. N., Kabir, M. Z. (1995). Shear strain effects in lateral stability of thin-walled fibrous composite beams. *Journal of Engineering Mechanics*, 121(5):640–647.

[8] Lee, J., Kim, S.-E. (2001). Flexural–torsional buckling of thin-walled I-section composites. *Computers & Structures*, 79(10):987–995.

[9] Lee, J., Kim, S.-E. (2002). Lateral buckling analysis of thin-walled laminated channel-section beams. *Composite Structures*, 56(4):391–399.

[10] Lee, J., Kim, S.-E., Hong, K. (2002). Lateral buckling of I-section composite beams. *Engineering Structures*, 24(7):955–964.

[11] Cortínez, V. H., Piovan, M. T. (2002). Vibration and buckling of composite thin-walled beams with shear deformability. *Journal of Sound and Vibration*, 258(4):701–723.

[12] Shan, L., Qiao, P. (2005). Flexural–torsional buckling of fiber-reinforced plastic composite open channel beams. *Composite Structures*, 68(2):211–224.

[13] Cortínez, V. H., Piovan, M. T. (2006). Stability of composite thin-walled beams with shear deformability. *Computers & Structures*, 84(15-16):978–990.

[14] Kim, N.-I., Shin, D. K., Kim, M.-Y. (2007). Improved flexural–torsional stability analysis of thin-walled composite beam and exact stiffness matrix. *International Journal of Mechanical Sciences*, 49(8):950–969.

[15] Kim, N.-I., Shin, D. K. (2009). Dynamic stiffness matrix for flexural-torsional, lateral buckling and free vibration analyses of mono-symmetric thin-walled composite beams. *International Journal of Structural Stability and Dynamics*, 9(03):411–436.

[16] Vo, T. P., Lee, J. (2009). On sixfold coupled buckling of thin-walled composite beams. *Composite Structures*, 90(3):295–303.

[17] Vo, T. P., Lee, J. (2009). Flexural–torsional coupled vibration and buckling of thin-walled open section composite beams using shear-deformable beam theory. *International Journal of Mechanical Sciences*, 51 (9-10):631–641.

[18] Nguyen, T.-T., Thang, P. T., Lee, J. (2017). Flexural-torsional stability of thin-walled functionally graded open-section beams. *Thin-Walled Structures*, 110:88–96.

[19] Nguyen, T.-T., Thang, P. T., Lee, J. (2017). Lateral buckling analysis of thin-walled functionally graded open-section beams. *Composite Structures*, 160:952–963.

[20] Nguyen, T.-T., Lee, J. (2018). Flexural-torsional vibration and buckling of thin-walled bi-directional functionally graded beams. *Composites Part B: Engineering*, 154:351–362.

[21] Nguyen, N.-D., Nguyen, T.-K., Vo, T. P., Nguyen, T.-N., Lee, S. (2019). Vibration and buckling behaviours of thin-walled composite and functionally graded sandwich I-beams. *Composites Part B: Engineering*, 166:414–427.

[22] Lee, J. (2001). Center of gravity and shear center of thin-walled open-section composite beams. *Composite Structures*, 52(2):255–260.

[23] Lee, J. (2005). Flexural analysis of thin-walled composite beams using shear-deformable beam theory. *Composite Structures*, 70(2):212–222.

[24] Lee, J., Lee, S.-h. (2004). Flexural–torsional behavior of thin-walled composite beams. *Thin-Walled Structures*, 42(9):1293–1305.

[25] Nguyen, T.-T., Kim, N.-I., Lee, J. (2016). Analysis of thin-walled open-section beams with functionally graded materials. *Composite Structures*, 138:75–83.

[26] Nguyen, T.-T., Kim, N.-I., Lee, J. (2016). Free vibration of thin-walled functionally graded open-section beams. *Composites Part B: Engineering*, 95:105–116.

[27] Lee, J., Kim, S.-E. (2002). Free vibration of thin-walled composite beams with I-shaped cross-sections. *Composite Structures*, 55(2):205–215.

[28] Sheikh, A. H., Asadi, A., Thomsen, O. T. (2015). Vibration of thin-walled laminated composite beams having open and closed sections. *Composite Structures*, 134:209–215.

[29] Nguyen, N.-D., Nguyen, T.-K., Vo, T. P., Thai, H.-T. (2018). Ritz-based analytical solutions for bending, buckling and vibration behavior of laminated composite beams. *International Journal of Structural Stability and Dynamics*, 18(11):1850130.

[30] Li, J., Huo, Q., Li, X., Kong, X., Wu, W. (2014). Vibration analyses of laminated composite beams using refined higher-order shear deformation theory. *International Journal of Mechanics and Materials in Design*, 10(1):43–52.